Performance Design and Testing of Propeller for Shallow-Fishery and Tailing Thai Boat: 2-blade type
Part (2) : A method for optimum cavitation of ship propeller

J. Charoensuk[1], J. Noosomton[2]

Faculty of Engineering, King Mongkut's Institute of Technology Ladkrabang, Bangkok, Thailand, 10520
[1]E-mail; kcjarruw@kmitl.ac.th, Tel. (66)-0-2326-9987, Fax. (66)-0-2326-9053
[2]E-mail; imcjrn@src.ku.ac.th, Tel. (66)-38-352606-10 Ext.2679, Fax. (66)-38-352607

Abstract

This paper presents a method for optimized cavitation of 2-blade type ship propeller. A practical method was achieved by combining a vortex lattice lifting method and lifting surface method. The optimum circulation distribution yielding the maximum lift-to-torque ratio was computed for given thrust and chord lengths along the radius of the propeller by dividing the blade into a number of panels extending from hub to tip. The radial distribution of bound circulation could be computed by a set of vortex elements that have constant strengths. A discrete trailing free vortex line was shredded at each of the panel boundaries whose strength equal to the difference in strengths of the adjacent vortices. The vortex system was built from a vortex element, each consisting of a bound vortex segment of constant strength and 2 free vortex lines of constant strengths. A Finite differential equation could be formulated by using these vortex systems.

Keywords: Optimum Ship Propeller, Propeller Design, Cavitations Number

1 INTRODUCTION

Cavitation flows are highly complicate because it is a rapid phase change phenomenon, which often occurs in the high-speed or rotating fluid machineries. It is well known that the cavitating flows is of great interest. Numerical method is highly important approach for studying the cavitating flow. Computational methods for cavitation have been studied since over two decades ago. In general, the methods can be largely categorized into two groups, Single-phase modeling with cavitation interface tracking and multi-phase modeling with cavitation interface capturing.

The former approach has been widely adopted for in viscid flow solution methods, such as potential flow boundary element methods. It assumes the cavitation region as a large bubble with a distinct liquid/vapor interface. Basically three assumptions are made for a cavitation bubble; the bubble boundary is a free surface; the pressured inside the bubble is constant and equals to the vapor pressure of is corresponding liquid; the closure region of the bubble can be approximated by a wake model. Third assumption is prime limitation of the method. The computation accounts only for the liquid phase; grid is often regenerated iteratively to conform to the cavity shape. This method is capable of simulating sheer cavitation but may not be adequate for cases in which bubble growth and detachment exists. In addition, so far, they are limited to two dimensional planar or axis-symmetric flows because of the difficulties involved in tracking three dimension interfaces, In Kinnas and Fine (1992) and Fine and Kinnas (1993), a low order potential-based boundary element method (BEM) was introduced for the nonlinear analysis of three-dimensional flow around cavitating propellers subjected to nonaxisymmetric inflows. The method was later extended to predict leading-edge and midchord partial cavitation on either the face or the back of the blades (Mueller and Kinnas, 1999).

The latter approach can be adopted for viscous flow solution method, such as the RANS equation solvers, and is very popular in the cavitation research recently. The cavitating flow is treated as the homogeneous equilibrium single-fluid flow which satisfies Navies-Stokes equation. The key challenge is how to define the mixed density of the single-fluid. In general, the cavitation modeling can be largely categorized into two groups according the relation that defines the variable density field. One cavitation modeling is based on the equation of state that relates pressure and density. By assuming the cavitating process to be isothermal, mixed density is simply a function of local pressure. Hoeijmakers and Kwan (1998) adopted a sine law to simulate the cavitating flow around two dimensional hydrofoils with Euler equation, and the computational results of surface pressure coefficient are in good agreement with experimental data. Chen and Heister (1996) derived a time and pressure dependent differential equation for density. Qiao Qin (2003) used fifth-order polynomial of pressure to define the mixed density. The other cavitation modeling is to introduce the concept to volume fraction, and then the mixed density is calculated using the volume fraction. Kubota, et al. (1992) coupled the Rayleigh-Plesset equation to compute the volume fraction based on the bubble radius, A mass transport equation cavitation model has been recently developed Shin Hyung Rhee and Kawamura (2003) Studied the cavitating flow around a marine propeller using an unstructured mesh with FLUENT 6.1. The cavitating propeller performance as well as cavitation inception and cavity bubble shape were in good agreement with experiment measurements and observation. In addition, Francesco Salvatore (2003) developed a hybrid viscous/inviscous approach for the analysis of marine propeller cavitation.

In this paper, the cavitating performance and open water performance of Shallow-Fishery and Tailing Thai Boat was numerically simulated. The effect of non-condensable gas mass fraction of predicted cavitating performance was mainly studied. The predicted cavity shapes were in good agreement with comparison the local domestic propeller. Which the shallow-fishery and tailing Thai boat used low-diesel engine by the researcher observation and result on open literature.

2 DESCRIPTIONS AND NUMERICAL METHOD

2.1 Blade Performance

We consider rotating with the velocity of U_T in a uniform axial velocity of *U*. The blade spacing *h* is assumed to be sufficiently small as compared with the blade length *l* and the flow in the blades. The axial and tangential velocity disturbances are represented by δu_1 and δv_1, respectively, at the inlet, and the axial velocity disturbance δu_2 at the outlet. The cavity of volume V_C per blade appears at the inlet. The velocity triangle at the inlet is shown in Figure 1.

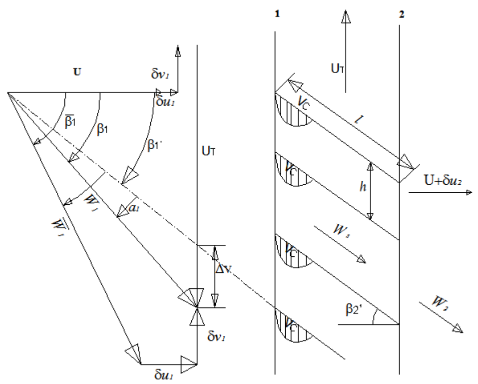

Figure 1. Rotor and Inlet Velocity Triangle

It is assumed that all of the cavitation can be lumped into the volume V_C upstream of the blade passage, and that the subsequent rotor flow can be modeled as single-phase incompressible liquid flow (the more complex blade passage nodel of Brennen[9] suggests that this is a good first approximation). Then the unsteady Bernoulli's equation applied to the relative flow in the rotor yields.

$$\frac{p_2 - p_1}{\rho} \equiv \frac{1}{2}(W_1^2 - W_2^2) - \frac{\partial'}{\partial t'}(\phi_2 - \phi_1) - \frac{\Delta p_t}{\rho} \qquad (1)$$

Here,

$$\frac{\partial'}{\partial t'} = \frac{\partial}{\partial t} + U_T \frac{\partial}{\partial y}$$

It is a time derivative in a frame rotating with the rotor, if β' is the average blade angle, as show in Figure 1, the difference of the velocity potential can be approximated by

$$\phi_2 - \phi_1 = \int_1^2 W_S ds \cong \frac{u_2 l}{\cos\beta'}$$

The total pressure loss Δp_t in the blades in represented by two coefficients, ζ_Q and ζ_S

$$\frac{\Delta p_t}{\rho} \equiv \zeta_Q (U + \delta u_1)^2 + \zeta_S (\Delta V)^2 \qquad (2)$$

Where ΔV is the incidence velocity as show in Figure 1. and can be expressed as

$$\Delta V = (U + \delta u_1)(\tan\overline{\beta_1} - \tan\beta_1')$$

Thus ζ_Q represents the hydraulic loss in the blade passage, and ζ_S the incidence loss at the inlet. The differences between pressure fluctuations upstream and downstream of the impeller are obtained by considering Eqs.(1) and (2) after linearization to yield

$$\frac{\delta p_2 - \delta p_1}{\rho U^2} = (1 - L_U)\frac{\delta u_1}{U} - (\tan\overline{\beta_1} + L_V) \frac{\delta v_1}{U} - \frac{1}{\cos_2 \beta_2'}\frac{\delta u_2}{U} - \frac{1}{\cos\beta'}\frac{1}{U}\frac{\partial'}{\partial t'}\left(\frac{\delta u_2}{U}\right) \qquad (3)$$

Where L_u and L_v are given by

$$L_u = \frac{\partial \Delta p_t}{\partial(\rho U u 1)} = 2\zeta_Q + 2\zeta_S \tan\beta_1' \cdot (\tan\beta_1' - \tan\overline{\beta_1})$$

$$L_v = \frac{\partial \Delta p_t}{\partial(\rho U v 1)} = 2\zeta_S (\tan\beta_1' - \tan\overline{\beta_1})$$

In general, cavitation instabilities appear at larger cavitation number than those which brings about significant deterioration in the pressure performance. Therefore, the effect of cavitation on the pressure rise across the rotor has been omitted from the present analysis and is not included in Eq.(3).

2.2 Cavitation Model and Numerical Method

The cavitation model employs in the study is based on the so called "Full Cavitation Model" by Singhal et.al.[14], This model accounts for all first order effects, i.e. phase change bubble dynamics, turbulent pressure fluctuations and non-condensable gases. This model is under the framework of multi-phase flows and has the capability of accounting for the effects of slip velocity been liquid and gaseous phases[15]. The main part of every cavitation physical model is to find the mass transfer equation between the liquid and vapor phases which in the study is as follows:

$$\frac{\partial}{\partial t}(\rho_m f_v)+\nabla\cdot(\rho_m \vec{v}_v f_v)= \nabla\cdot\left(\frac{\mu_t}{\sigma_v}\nabla\cdot f_v\right)+R_e-R_c \tag{4}$$

The source terms in Eq.(4) R_e and R_c are to be related to the bubble dynamics and vapor volume fraction. To account for the bubble dynamics, the reduce equation is employed as for many other study in the same modeling category. Following the approach used by Singhal et.al.[14], and considering the limiting bubble size with assuming that the typical bubble diameter is the same as the maximum possible bubble size, the expressions for R_e and R_c ate obtained as:

$$R_e = C_e \frac{v_{ch}}{\gamma}\rho_v\rho_l\sqrt{\frac{2}{3}\frac{p_{sat}-p}{p_l}}(1-f_v), \quad p<p_{sat} \tag{5}$$

And

$$R_c = C_c \frac{v_{ch}}{\gamma}\rho_l\rho_l\sqrt{\frac{2}{3}\frac{p-p_{sat}}{p_l}}f_v, \quad p>p_{sat} \tag{6}$$

Where C_e and C_c are two empirical constants, after careful study of the numerical stability and physical behavior of the solution. Their values are adopted in the study. The effects of turbulence induced pressure fluctuations are taken into account by raising the phase change threshold pressure from p_{sat} to p_v, which is written as:

$$p_v = p_{sat} + 0.5p'_{turb.} \tag{7}$$

It is widely acknowledged that the effects of non-condensable gases need to be taken into account, as the operating liquid usually contains small finite amounts of such gases, e.g. dissolved gases and aeration. The working fluid is assumed to be a mixture of liquid and the gaseous phases, with the gaseous phase being comprised of liquid vapor and non-condensable gas. The mixture density is calculated as:

$$\rho_m = \alpha_v\rho_v + \alpha_g\rho_g + (1-\alpha_l-\alpha_g)\rho_l \tag{8}$$

Considering all these effects, Eq.(5),(6) can be rewritten as:

$$R_e = C_e \frac{\sqrt{k}}{\gamma}\rho_v\rho_l\sqrt{\frac{2}{3}\frac{p_v-p}{p_l}}(1-f_v-f_g), \quad p<p_v \tag{9}$$

and

$$R_c = C_c \frac{\sqrt{k}}{\gamma} \rho_l \rho_l \sqrt{\frac{2}{3} \frac{p - p_v}{p_l}} f_v, \quad p > p_v \tag{10}$$

The finite volume method which allows the use of computational element with an arbitrary polyhedral shape. Convective terms are discredited using the second order accurate upwind scheme, which diffusive terms ate discredited using the second order accurate central differencing scheme. The cavity volume V_c per blade and per unit span is normalized using the blade spacing h and represented by a functions.

$$a(\sigma, \alpha_1) \equiv \frac{V_c}{(h^2 \times 1)} \tag{11}$$

Under quasi-steady conditions, the non-dimensional cavity volume a is considered to be a function of the incident angle α_1 and the inlet cavitation number σ defined as follows

$$\sigma = \frac{p_1 - p_v}{\rho W_1^2 / 2} \tag{12}$$

When p_1, p_v and W_1 are the inlet pressure, the vapor pressure, and the inlet relative velocity, respectively. Then as originally suggested by Brennen and Acosta[10] the change of cavity volume, δV_C is related to the deviations δW_1, δp_1 and $\delta\alpha_1$ by,

$$\delta V_C = h^2 \left[\frac{\partial a}{\partial \sigma} \left(\frac{\partial \sigma}{\partial W_1} \partial W_1 + \frac{\partial \sigma}{\partial p_1} \partial p_1 \right) + \frac{\partial a}{\partial \alpha_1} \partial \alpha_1 \right] \tag{13}$$

From the velocity triangle show in Figure 1. the deviations δW_1 and $\delta\alpha_1$ can be represented in terms of the deviations δu_1 and δv_1 from the uniform axial velocity. Then Eq.(13) may be written as

$$\delta V_C = h^2 \left[F_1 \cdot \left(\frac{\delta u_1}{U} \right) + F_2 \cdot \left(\frac{\delta v_1}{U} \right) + F_3 \cdot \left(\frac{\delta p_1}{\rho U^2} \right) \right] \tag{14}$$

where

$$F_1 = 2\sigma K \cos^2 \overline{\beta_1} - M \sin \overline{\beta_1} \cos \overline{\beta_1}$$

$$F_2 = -2\sigma K \sin \overline{\beta_1} \cos \overline{\beta_1} - M \cos^2 \overline{\beta_1}$$

$$F_3 = -2K \cos^2 \overline{\beta_1}$$

And

$$M = \frac{\partial a}{\partial \alpha_1}, \quad K = -\frac{\partial a}{\partial \sigma} \tag{15}$$

When M and K are the mass flow gain factor and cavitation compliance, respectively. For the evaluation of these factors, Refer Brennen[11][12] and Otsuka, et al.[13] The continuity relation across the impeller is

$$h = (\delta u_2 - \delta u_1) = \left(\frac{\partial'}{\partial t'} \right) \delta V_C \tag{16}$$

Where subscritipts 1,2 indicate the inlet and outlet of the impeller. By combining Eqs.(14),(16), the continuity equation can be expressed as follows,

$$\delta u_2 - \delta u_1 = h \left(\frac{\partial'}{\partial t'} \right) \left[F_1 \cdot \left(\frac{\delta u_1}{U} \right) + F_2 \cdot \left(\frac{\delta v_1}{U} \right) + F_3 \cdot \left(\frac{\delta p_1}{\rho U^2} \right) \right] \tag{17}$$

With cavitation, it serves as a compliant element and it is not needed to have an explicit compliant element as the simplest model of cavitation surge, we consider a system composed of an inlet pipe with the length *L*, and outlet pipe with infinite length. The last simplifying assumption suggests that there would be no flow rate fluctuation downstream of the rotor, $\delta u_2 = 0$. In addition to this we can apply the moment equation of the fluid in the inlet pipe, Eq.(18),

$$\delta p_1 = -\rho U \delta u_1 - \rho L \left(\frac{d}{dt} \right) \delta u_1 \qquad (18)$$

The continuity equation across the rotor, Eq.(16) with $\frac{\partial'}{\partial t'} = \frac{\partial}{\partial t}$ so, $h(\delta u_2 - \delta u_1) = \left(\frac{\partial}{\partial t} \right) \delta V_C$

And the cavitation characteristics of Eq.(14) with $\delta v_1 = 0$

and

$$\delta V_C = h^2 \left[F_1 \cdot \left(\frac{\delta u_1}{U} \right) + F_3 \cdot \left(\frac{\delta p_1}{\rho U^2} \right) \right]$$

By combining these equations, we obtain the following result.

$$\frac{d^2}{dt^2} \left(\frac{\delta u_1}{U} \right) - \frac{F_1 - F_3}{F_3 (L/U)} \frac{d}{dt} \left(\frac{\delta u_1}{U} \right) - \frac{U^2}{F_3 L h} \left(\frac{\delta u_1}{U} \right) = 0 \qquad (19)$$

Since $F_3 = -2K\cos^2 \overline{\beta_1} < 0$, negative damping occurs when $F_1 - F_3 < 0$ and this leads to the onset condition of cavitation surge

$$M > 2(1+\sigma)\phi K \qquad (20)$$

From Eq.(19) gives the cavitation surge frequency

$$f = \frac{1}{2\pi} \frac{U}{\sqrt{-F_3 L h}} = \frac{U_T}{2\pi \sin \overline{\beta_1}} \frac{1}{\sqrt{2KLh}} = \frac{1}{2\pi} \frac{1}{\sqrt{\rho C L}} \qquad (21)$$

Where the last expression is obtained with,

$$C = -\frac{F_3 h}{(\rho U^2)} = \frac{2\sin^2 \overline{\beta_1} K h}{(\rho U_T^2)}$$

This shows that the frequency is the nature frequency of the inlet pipe-cavitation system and is proportional to the blades speed, caused by the fact that the compliance *C* is correlated with the tip speed. This is quite different from the frequency of normal surge, which is fixed to the natural frequency of the system. The above results were obtained not by using the pressure performance of the blades Eq.(3) but by using only the continuity across the rotor Eq.(16) and the cavitation characteristics Eq.(14) the criterion for normal surge it the positive slope of the pressure performance, it is the cause of normal surge. If the flow rate is increased, the pressure difference across the pump is increased and this accelerates the flow through the pump. This positive feedback through the performance is the cause of normal surge. On the other hand, the criterion for cavitation surge, Eq.(20) shows that positive mass flow gain factor, *M>0*, is the cause of cavitation surge. When the flow rate is increased, the incidence angle α_1 to the rotor blade is decreased. If $M = \partial(V_C/h)/\partial\alpha_1$ is positive, the cavity volume V_C is decreased.

Then the upstream flow rate is increased to fill up the space once occupied by the cavity. This positive feedback through the continuity relation is the cause of cavitation surge. So, the mechanism of normal surge and cavitation surge is totally different.

3 RESULTS AND DISCUSSIONS

The main purpose of testing the propeller models in the water tunnel of type new-design and type local domestic in Thailand Table(1) for comparison behavior of occur bubble and test efficiency is determination of the characteristic curves under cavitation and non-cavitation conditions, usually characteristic curves are variations of thrust and torque coefficients, with respect to the advance coefficient. In obtaining the characteristic curves Figures (2),(3) the rotational speed is kept constant and advance velocity is varied in the range of allowable water tunnel flow speed (e.g., in the current water tunnel, 0 - 3.5 m/s). Thus, different values for the advance coefficient are obtained. In the non-cavity test, the static pressure is constant at the value of the usual operating pressure.

Table 1. Principal particular of new design Model-A, model-B and Model-C (Local type)

Model Name	Model-A (2-20-35)	Model-B (2-20-50)	Model-C (Local)
Number of blades	2	2	2
Diameter (m)	0.24	0.24	0.25
P/D	0.940	0.940	-
$EAR=A_E/A_O$	0.35	0.50	~0.35
Skew Angle (degree)	20	20	~21
Cavity at 0.7R	1.5662691	1.5662691	-

The reason behind the above mentioned procedure lies in the type of dimensional analysis that is used for deriving non-dimensional coefficients in characteristic curves. The necessary dimensional analysis for open water conditions has been stated.

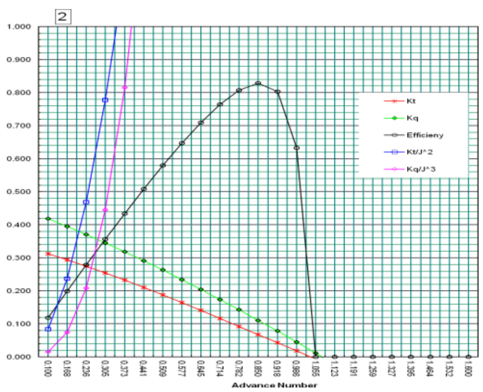

Figure 2. Characteristic curve of model A;

(B2-20-35)

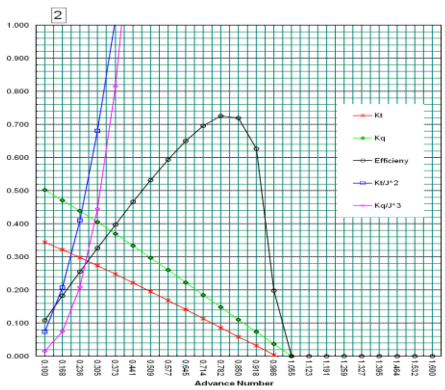

Figure 3. Characteristic curve of model B;

(B2-20-50)

In cavitation tests, two kinds of curves are derived. One is the characteristic curve in a constant cavitation number, which is used to show the deviation of torque and thrust from a non-cavitating state. The second is the diagram of torque and thrust coefficients on the basis of the cavitation number, which is used to show the cavitation breakdown analysis. In cavitation tests, the static pressure and advance velocity inside the cavitation tunnel test section ate lowered gradually in order to sketch the required diagrams.

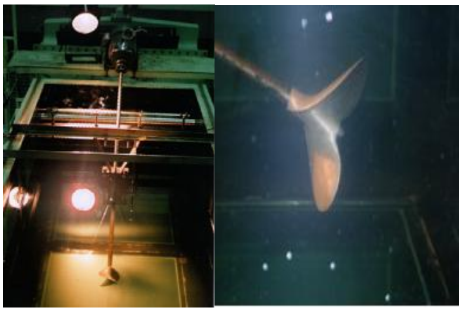

Figure 4. Installation of Tailing Thai Boat Type Local Domestic at Lab. Water Tunnel

The result of testing the model A,B and C propeller in non-cavitation states and at two rotational speeds of 865 and 1000 rpm are depicted in Figures (4),(5),(6),(7),(8) and (9) respectively. Axial velocity is varied from 0.3 to 3.5 m/s. it is seen that, at low values of J, there is an appreciable difference between the results. This is a general fact because according to the definition, K_t is proportional to the first power of thrust rather than the second power of rotational speed in the denominator. The testing of propellers for non-cavitation conditions is essential before proceeding to cavitating conditions. Firstly, using these results, the numerical method is validated for simulation of the fluid flow around the propeller models; secondly, solving the flow fields in non-cavitating conditions is used as the initial condition for propeller cavitation simulations which will be presented in the next paper.

The characteristic curve in cavitation and cavitation free conditions are compared in Figure.(2),(3) for a rotational speed of 1185 rpm. (New design) in the cavitation condition. Similar experiments are carried out at 865 rpm. These data are used as benchmarks experimental work for the present research these. for propeller model A; type 2 blades skew angle 20 degree and developed area 35 (B2-20-35) and propeller model B; type 2 blades skew angle 20 degree and developed area 50 (B2-20-50).

The quantitative investigation of cavitation has been carried out; and now, it is investigated qualitatively as given in Figures.(5),(6),(7),(8) and (9) respectively. The pictures shows cavitation at 865 rpm and at an axial velocity of 2.5 m/s. The photographs in Figure.(5) the cavitation surface is glassy smooth and the propeller blade surface is seen clearly behind the cavitating surface. Thus, it is deduced that the formed cavitation is the sheet cavitation. It is seem that the photographs in Figure.(9) The propeller model C is also tested at 1000 rpm with a cavity greater developed full area.

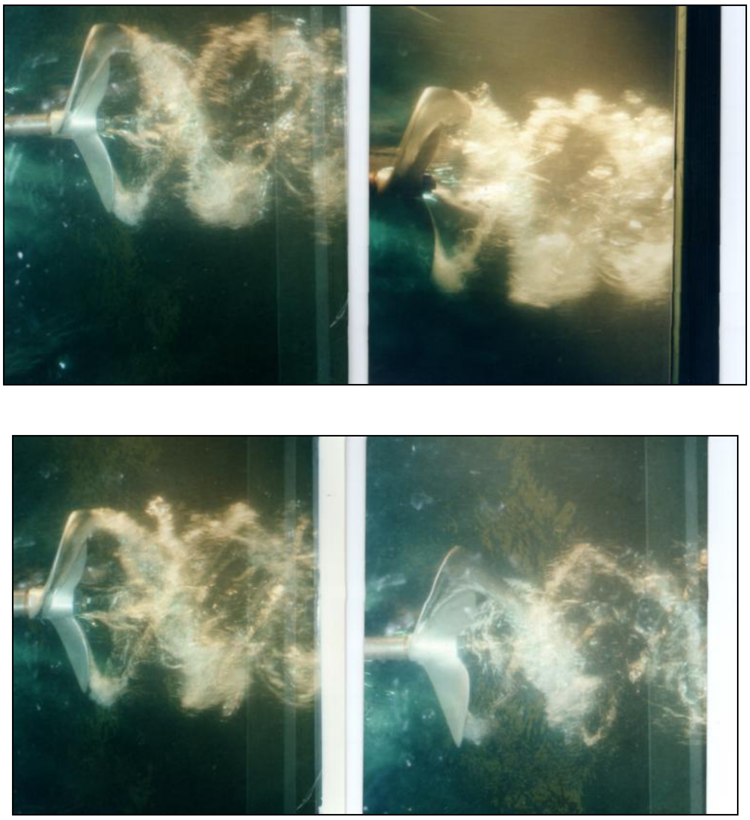

Figure 5. Illustration of propeller cavitation type local at rotational speed of 865 rpm

The photographs in Figure.(6) show cavity Appearance of propeller 2 blade skew angle 20 degree developed area 35,(B2-20-35) Velocity 865 rpm., Type new design for Shallow-Fishery and Tailing Thai Boat, An example of sequence by camera at the time when impulsive force was measured.

Figure 6. Illustration of propeller cavitation type new design at rotational speed of 865 rpm

The photographs in Figure.(7) show cavity Appearance of propeller 2 blade Velocity 865 rpm., Type local domestic for market Shallow-Fishery and Tailing Thai Boat, An example of sequence by camera at the time when impulsive force was measured.

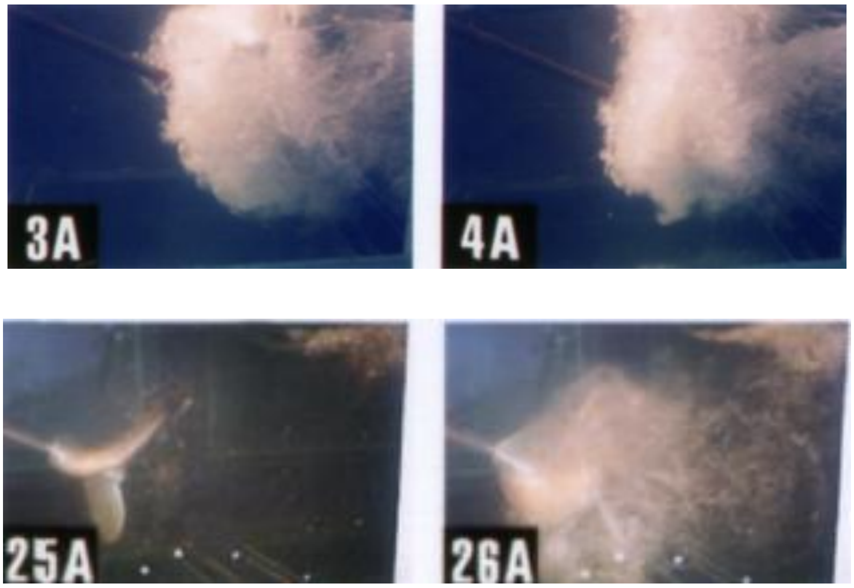

Figure 7. Illustration of propeller cavitation type local at rotational speed of 865 rpm developed area 50

The photographs in Figure.(8) show cavity Appearance of propeller 2 blade skew angle 20 degree developed area 50,(B2-20-50) Velocity 865 rpm., Type new design for Shallow-Fishery and Tailing Thai Boat, An example of sequence by camera at the time when impulsive force was measured.

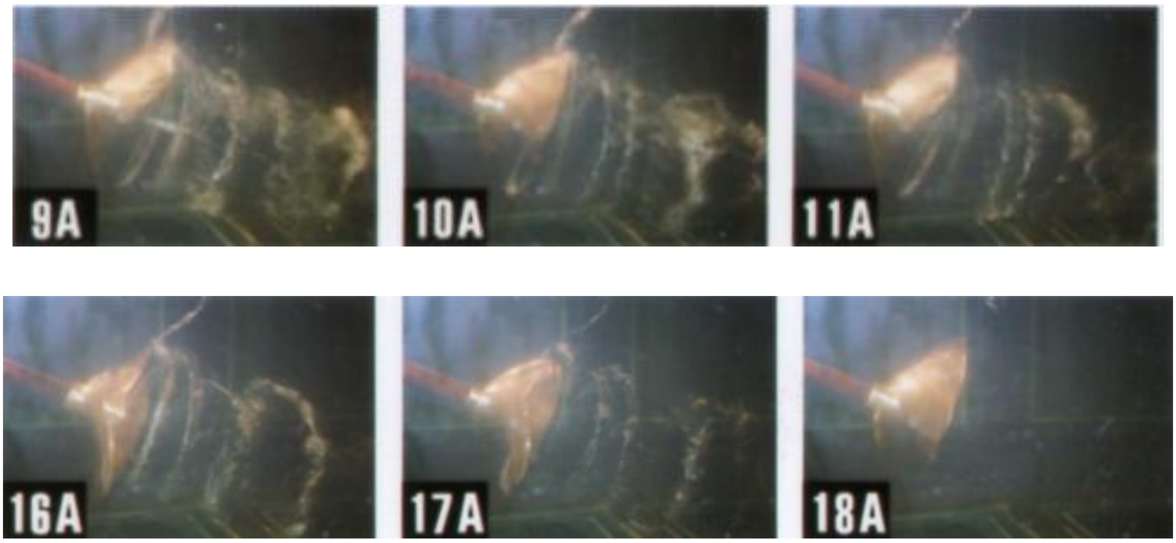

Figure 8. Illustration of propeller cavitation type new design at rotational speed of 865 rpm, (B2-20-50)

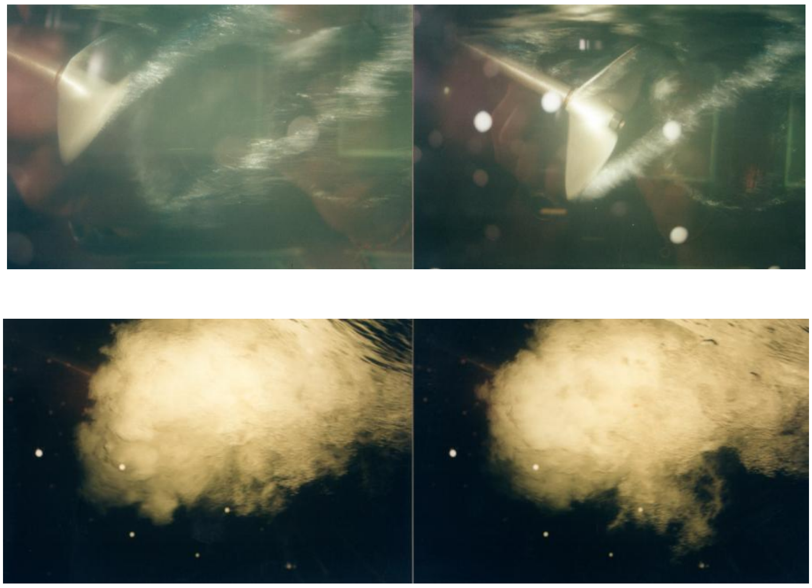

Figure 9. Cavitation full developed at Velocity 1000 rpm. Type Local Domestic

4 CONCLUSIONS

In this paper, cavitation flow is investigated experimentally on two conventional for shallow-fishery and tailing Thai boat. The preliminarily experimental result show better performance, when compared with local domestic type.

The cavitating performance and open water performance of Shallow-Fishery and Tailing Thai Boat has been numerically investigated using a mesh based FLUENT solver with a Full Cavitation model based on transport equation and standard *k*-ω turbulent. The achievement of this investigation will be presented in the next publication. The overall results suggest that the present approach is practicable as a design approach for low speed propeller for Thailand fishery industry.

NOMENCLATURE

Cp = Pressure coefficient

$C_P = (P - P_O)/0.5\rho n^2 D^2$ for propeller

$C_P = (P - P_O)/0.5\rho U_\infty^2$ for otherwise

J_S = Advance ratio based on V_s ,

$J_S = V_S / nD$

K_Q = Torque coefficient, $K_Q = Q / \rho n^2 D^5$

K_T = Thrust coefficient, $K_T = T / \rho n^2 D^4$

n = Propeller rotational frequency (rev/sec)

P_o = Far upstream pressure, at the propeller Axis

P_{sat} = liquid saturated pressure (Pascal)

P_v = Vapor pressure of water

p, q = Field point and variable point

$\vec{q}_t$ = Total velocity

Q = Propeller torque

T = Propeller thrust

$\vec{U}_{in}$ = Local inflow velocity (in the propeller fixed system)

$\vec{U}_w$ = Effective inflow velocity (in the ship fixed system)

Vs = Ship speed

$\vec{V}_{Tip}$ = Total velocity at the center of the tip vortex core

$\vec{V}_w$ = Total velocity on wake surface

ω = Propeller angular velocity

ρ = Fluid density

σ_n = Cavitation number based on *n*,

$$\sigma_n = (P_O - P_v)/0.5\rho n^2 D^2$$

σ_v = Cavitation number based on *Vs* ,

$$\sigma_n = (P_O - P_v)/0.5\rho V_s^2$$

ACKNOWLEDGEMENTS

The authors would like to thank Captain Sarawut Wongchenyour (RTN.), Royal Thai Navy for contributions toward this work.

This work is supported by ANSYS Software at KMIT'L.

REFERENCES

[1] Francisco Pereira et.al., "Experimental and Numerical Investigation of the Cavitation Pattern on a Marine Propeller",[C]. 24th Symposium on Naval Hydrodynamics, Fukuoka, Japan, 8-13 july, 2002.

[2] Francesco Salvatore et al., "A Viscous / Inviscous Coupled Formulation for Unsteady Sheet Cavitation Modelling of Marine Propellers",[C]. 5th International Symposium on Cavitation, Osaka, Japan 1-4 November, 2003.

[3] Hoeijmakers. H.W.M, Janaaens. M.E, Kwan. W, "Numerical Simulation of Sheet Cavitation",[C].3rd International Symposium on Cavitation Grenoble France, 1998.

[4] Inanc Senocak, Wei Shyy, "Numerical Simulation of Turbulent with Sheet Cavitation",[C].4th International Symposium on Cavitation, SessionA7.002, 2001.

[5] Inanc Senocak, Wei Shyy, "A Pressure-Based Method for Turbulent Cavitating Flow Computation", [J]. Journal of Computational Physics,Vol.176,pp.363-383, 2002.

[6] Kubota A, Kato H, Yamaguchi H, "A new Modeling of Cavitating Flows: A Numerical Study of Unsteady Cavitation on A Hydrofoil Section",[J]. Journal of Fluid Mechanics, Vol.240, pp.59-96, 1992.

[7] Amdt,R., "Cavitation in vertical Flows", Annu. Rev. Fluid Mech., Vol.34, pp.143-175, 2002.

[8] Tsujimoto Y., Kamijo K.,and Brennen C.E., "Unified Treatment of Flow Instabilities of Turbo machines", AIAA Journal of Propulsion and Power, Vol.17, No.3, pp.636-643, 2001.

[9] Brennen C.E., "The bubbly Flow Model for the Dynamic Characteristics of Cavitating Pump",[J]. Journal of Fluids Mechanics, Vol.89, No.2, pp.223-240, 1978.

[10] Brennen C.E., and Acosta A.J., "The Dynamic Transfer Function for a Cavitating Inducer", ASME Jorunal of Fluids Engineering, Vol.98, No.2, pp.182-191, 1976.

[11] Brennen C.E., "Hydrodynamics of Pumps", Oxford University Press and Concepts ETI, Inc., Oxord, England, U.K., 1994

[12] Brennen C.E., Meissner C., Lo E.Y., and Hoffmann G.S.,"Scale Effects in the dynamic Transfer Functions for Cavitating Inducers", ASME Journal of Fluid Engineering, Vol.118, No.2, pp.400-408, 1996.

[13] Otsuka S., Tsujimoto Y., Kamijo K., Furuya O.,"Frequency Dependence of mass Flow Fain Factor and Cavitation Complicance of Cavitating Inducers", ASME Journal of Fluid Engineering, Vol.118, No.4, pp.400-408, 1996.

[14] Singhal A.K., Athavale M.M., Li H. and Jiang Y., "Mathematical basis and validation of the full cavitation Model", ASME Journal Fluids Engineering, Vol.124, pp.617-624, 2002

[15] Rhee S.H., Kawamura T., and Li H., "Propeller cavitation study using an unstructured grid based Navier-Stoker solver", ASME Journal Fluids Engineering, Vol.127, pp.986-994, 2005